

# Constrained High Accuracy Stereo Reconstruction Method for Surgical Instruments Positioning

Chenhao Wang<sup>1</sup>, Yi Shen<sup>1</sup>, Wenbin Zhang<sup>2</sup> and Yuncai Liu<sup>1</sup>

<sup>1</sup>Institute of Image Processing and Pattern Recognition, Shanghai Jiao Tong University  
Shanghai, China

<sup>2</sup>Department of Oral and Maxillofacial Surgery, Ninth People's Hospital,  
Shanghai Jiao Tong University School of Medicine  
Shanghai, China

[e-mail: chhwang007@gmail.com, zwb96493@hotmail.com]

\*Corresponding author: Chenhao Wang

*Received May 3, 2012; revised August 25, 2012; accepted September 21, 2012;  
published October 29, 2012*

---

## Abstract

In this paper, a high accuracy stereo reconstruction method for surgery instruments positioning is proposed. Usually, the problem of surgical instruments reconstruction is considered as a basic task in computer vision to estimate the 3-D position of each marker on a surgery instrument from three pairs of image points. However, the existing methods considered the 3-D reconstruction of the points separately thus ignore the structure information. Meanwhile, the errors from light variation, imaging noise and quantization still affect the reconstruction accuracy. This paper proposes a method which takes the structure information of surgical instruments as constraints, and reconstructs the whole markers on one surgical instrument together. Firstly, we calibrate the instruments before navigation to get the structure parameters. The structure parameters consist of markers' number, distances between each markers and a linearity sign of each instrument. Then, the structure constraints are added to stereo reconstruction. Finally, weighted filter is used to reduce the jitter. Experiments conducted on surgery navigation system showed that our method not only improve accuracy effectively but also reduce the jitter of surgical instrument greatly.

---

**Keywords:** high accuracy reconstruction, computer vision, surgical instruments positioning

## 1. Introduction

With the fast development of computer science, Surgical Navigation System (SNS) is widely used nowadays [1][2][3][4]. It registers the CT data to the operating space of the patient and tracking the surgical instruments in real time so that doctors can perform an operation referring to SNS. Therefore, it's quite important to improve the positioning accuracy as it determines the application accuracy directly.

Surgical instruments usually contain 3 markers and could be broadly categorized into 2 types. Probe instrument (Fig.1 (a)) has a probe point which touches the patient in surgical navigation. Non-probe instrument (Fig.1 (b)) doesn't have a probe point which is often used to establish reference coordinate system. Meanwhile, the instrument in Fig.1 (a) is a linear instrument whose markers are collinear. Markers are clearly shown in the binary image (Fig.1 (c)).

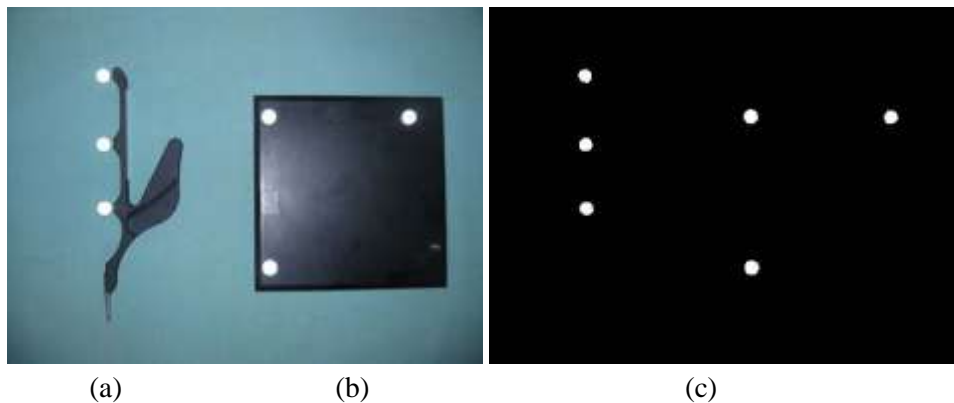


Fig. 1. Surgical instruments

(a) Probe instrument; (b) Non-probe instrument; (c) Binary image of instruments;

Usually, the problem of surgical instruments reconstruction is considered as the basic task in computer vision to estimate the 3-D position of an object from three pairs of image points in infrared light, which has been extensively explored and properly solved in literatures [5][6]. It's used by most existing system [6][7][8]. Recently, Duan et al. proposed an approach to surgical instruments positioning in visible light [12]. Although they have demonstrated some promising results on surgical instruments positioning, they still uses conventional stereo reconstruction algorithm and the markers are not sphere whose center will change in perspective. The disadvantage of conventional method is that it does not consider the structure information of surgical instruments. Meanwhile, the errors from light variation, imaging noise and quantization still affect the reconstruction accuracy. This paper proposes a method which takes the structure information of surgical instruments as constraints, and reconstructs the whole markers on one surgical instrument together. First, the method calibrates the instruments before navigation to get the structure parameters. The structure parameters consist of markers' number, distances between each markers and a linearity sign of each instrument. Then the structure constraints are added to stereo reconstruction. Moreover, weighted filter is used to reduce the jitter.

The rest of this paper is organized as follows. Conventional 3-D reconstruction algorithm is presented in section 2. High-accuracy 3-D structure reconstruction algorithm is proposed in section 3. Finally, experimental results on real data are reported in section 4, followed by conclusions in section 5.

## 2. 3-D Reconstruction Of Markers

In this section, we introduce the conventional 3-D reconstruction method [9] briefly.

First, the 2-D coordinates of each marker are obtained in bicameral. Next, we reconstruct the 3-D coordinates of these markers. The basic idea of 3-D a single marker's reconstruction is to use stereo imaging principle to calculate the 3-D coordinates of each marker, as shown in Fig. 2.

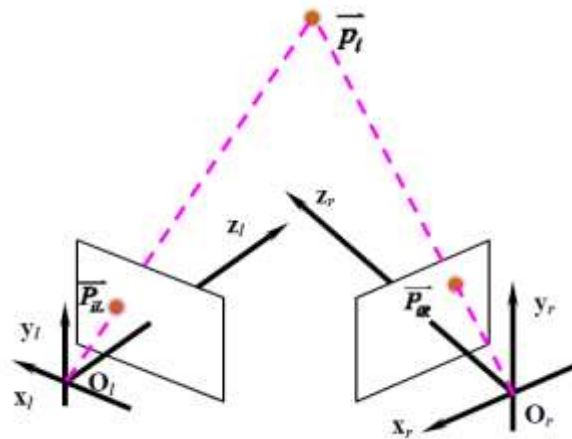


Fig. 2. Stereo Reconstruction

The projection function of binocular camera is:

$$\begin{cases} [A_L \quad \mathbf{0}] \bar{p}_i = \bar{P}_{iL} \\ [A_R \quad \mathbf{0}] [\mathbf{R}_0 \quad \mathbf{T}_0] \bar{p}_i = \bar{P}_{iR} \end{cases} \quad (1)$$

Where  $A_L$  and  $A_R$  are inner parameters matrix of left camera and right camera respectively;  $\mathbf{R}_0$  is rotation matrix from left camera to right camera;  $\mathbf{T}_0$  is translation matrix from left camera to right camera;  $\bar{P}_{iL} = (x_{iL} \ y_{iL} \ 1)^T$  is the homogeneous coordinate of the projection point position in left camera;  $\bar{P}_{iR} = (x_{iR} \ y_{iR} \ 1)^T$  is the homogeneous coordinate of the projection point position in right camera;  $\bar{p}_i = (x_i \ y_i \ z_i \ 1)^T$  is the homogeneous coordinate of a 3-D point.

$A_L$ ,  $A_R$ ,  $\mathbf{R}_0$ ,  $\mathbf{T}_0$  are obtained by camera calibration.  $\bar{P}_{iL}$  and  $\bar{P}_{iR}$  could be obtained by matching the points in the left and right cameras. Therefore,  $\bar{p}_i$  could be got by solving function (1).

The existing methods considered the 3-D reconstruction of the markers separately thus ignore the relationship between them. On the other hand, the errors from light variation, imaging noise and quantization affect the reconstruction accuracy.

### 3. 3-D Reconstruction Of Markers Based On Structure Constraints And Weighted Filter

In this section, we propose an innovative approach based on the structure constraints and weighting filter to improve the accuracy of the surgical instruments reconstruction. Firstly, surgical instruments have fixed structures and the distances between markers remain constant, so we can improve the reconstruction accuracy by combining the projection functions and the structure constraints together. Secondly, the motion of markers is continuous, thus we can filter to reduce the jitter tolerance.

Now we give the overall procedure of the proposed method.

Step 1: Obtain the structure information before navigation. For non-probe type instruments, we take the distances between the three markers as the structure parameters, those are  $d_{max}$  (the longest one),  $d_{mid}$  and  $d_{min}$  (the shortest one). For probe type instruments, we calculate not only the distances between the three markers as the structure parameters, but also the relationship between the probe point and the 3 markers for navigation.

Step 2: Reconstruct surgical instruments with structure constraints. For general surgical instruments, we add the distances constraints to projection function of binocular camera. For linear instruments, not only the distances constraints, but also the linear constraint should be added.

Step 3: Filter the image sequences. We predict the current value of each marker position, and calculate weighted mean of the predicted value and the reconstruction value got at Step 2.

#### 3.1 Structure Constraints

The structure information is obtained before navigation. It needs to be gained only once when a new instrument is added. The structure information is noted as points' number:  $n$ , points' distances:  $d_{1,2}, d_{1,3}, d_{1,4} \dots d_{2,3} \dots d_{n-1,n}$  (distances between markers) and a linearity sign of each instrument. The algorithm requires there are no same distances of each instrument.

The structure information can be obtained either by physical measurements such as calipers or be calculated using 3-D computer vision which we called instrument calibration. The physical measurements use calipers or other measure tools to obtain the distances between each center of markers. Since the structure of the instrument is often complex and the shape of the markers may be irregular, instrument calibration is a common method [7]. The method to calibrate the probe type and the non-probe type are different and we discuss them respectively.

For non-probe type instruments, we take the distances between the three markers as the structure parameters, those are  $d_{max}$  (the longest one),  $d_{mid}$  and  $d_{min}$  (the shortest one). The 3-D single point reconstruction algorithm is used to obtain the distances with different postures of the instrument. In order to reduce the error, we take the average of thousands of repeated calculations results as the final result.

For probe type instruments, we calculate not only the distances between the three markers as the structure parameters, but also the relationship between the probe point and the 3 markers for navigation. Since there is no marker on the probe point for detection, a special calibration method is adopted. We take the probe point as a fixed point, and then rotate the probe around it, as shown in Fig.3.

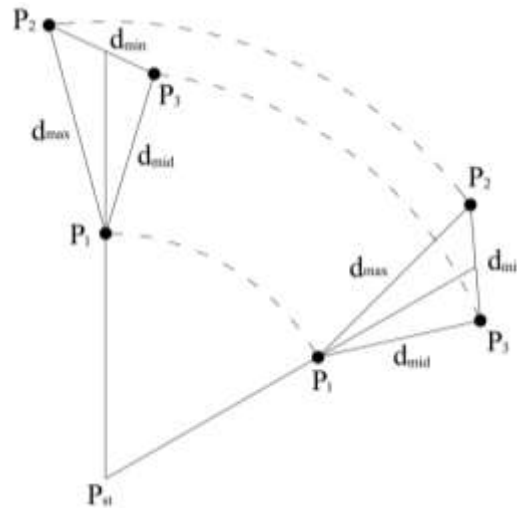


**Fig. 3.** Probe calibration principle

The coordinate of the  $i$ -th ( $i=1,2,3$ ) marker is denoted as  $\overline{p_{ij}} = (x_{ij} \ y_{ij} \ z_{ij})^T$  ( $j$  is serial number in the video,  $j=1\sim 5000$ ), the coordinate of the probe point is denoted as  $\rho_{is}$ , then the distance from  $\overline{p_{ij}}$  to  $\overline{p_{st}}$  is a constant, that is:

$$\|\overline{p_{ij}} - \overline{p_{st}}\| = \rho_{is} \quad (2)$$

The least square method [10] can be used to solve  $\overline{p_{st}}$ .

### 3.2 Markers' Classification

There is always more than one instrument in a surgery scene. Therefore we should identify the markers belong to which instrument. The method is to classify markers according to the distances between them:

- Calculate the distances between each marker.
- Compare the distances with the structure information. If the relative error is small than the allowable value, we mark both of the two markers to the same instrument.
- Check all the points belong to instrument  $i$  ( $1 < i < m$ ). If the points' number is not smaller than how many instrument  $i$  should have, calculate the distances between the markers to form an undirected graph. Check the path whether it belongs to instrument  $i$  by comparing the distances with the structure information, if not, delete the path. If the largest complete subgraph is equal to instrument  $i$ , the vertexes are the whole markers.

### 3.3 3-D reconstruction with structure constraints

For general surgical instruments, the structure constraints are the distances between the markers remain constant:

$$\|\overline{p_i} - \overline{p_j}\| = d_{i,j}, (1 \leq i < j \leq n) \quad (2)$$

Where  $d_{i,j}$  is the distance between  $\overline{p_i}$  and  $\overline{p_j}$ ,  $\overline{p_i}$  and  $\overline{p_j}$  are markers of surgical instrument.

Then the structure constraints are added to (1):

$$\begin{cases} [\mathbf{K}_L \quad \mathbf{0}] \bar{p}_i = \bar{P}_{iL}, (1 \leq i \leq n) \\ \mathbf{K}_R [\mathbf{R}_0 \quad \mathbf{T}_0] \bar{p}_i = \bar{P}_{iR}, (1 \leq i \leq n) \\ \|\bar{p}_i - \bar{p}_j\| = d_{i,j}, (1 \leq i < j \leq n) \end{cases} \quad (3)$$

For linear instruments, besides (2), the linear constraint should also be added:

$$\begin{cases} [\mathbf{K}_L \quad \mathbf{0}] \bar{p}_i = \bar{P}_{iL}, (1 \leq i \leq n) \\ \mathbf{K}_R [\mathbf{R}_0 \quad \mathbf{T}_0] \bar{p}_i = \bar{P}_{iR}, (1 \leq i \leq n) \\ \|\bar{p}_i - \bar{p}_j\| = d_{i,j}, (1 \leq i < j \leq n) \\ \bar{V}_{n,n-1} \times \bar{V}_{n,n-2} = \bar{\mathbf{0}} \\ \bar{V}_{2k,2k-1} \times \bar{V}_{2k,2k+1} = \bar{\mathbf{0}}, (1 \leq k \leq n/2) \end{cases} \quad (4)$$

Where  $\bar{V}_{i,j} = \bar{p}_i - \bar{p}_j$ .

Therefore, it becomes a nonlinear least squares problem and the Gauss-Newton iterative method [10] is suggested to solve (2) or (3) to get  $\bar{p}_i$ .

### 3.4 Weighted filter

Since the image sequences which are captured by binocular camera contain a wealth of information. Filtering algorithm and tracking algorithm can be used to improve the accuracy of surgical navigation. Although common filtering algorithm, such as median filtering, mean filtering, can effectively reduce noise, they are not suitable for real-time navigation systems for they will cause the navigation images hysteresis. This paper introduces a weighted filtering algorithm. Firstly, markers of surgical instruments's projection on 2D image are continuous and there trajectory on the 3D space is a 3D curve, so we get current position  $\bar{p}_i^F$  of by fitting marker trajectory. As Fig.4 showed, 15 frames are used to fit curve. We create a thread for fitting curves to ensure real-time nature of the algorithm. Secondly, we calculate weighted mean:

$$\bar{p}_i^W = \frac{\alpha \times \bar{p}_i + \beta \times \bar{p}_i^F}{\alpha + \beta} \quad (5)$$

Where  $\alpha$ ,  $\beta$  are weights.

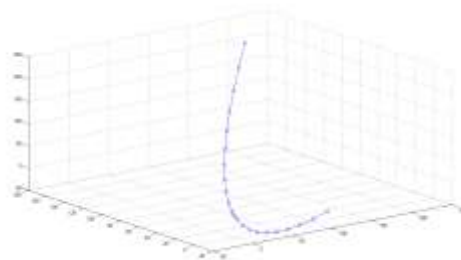


Fig. 4. Point trajectory fitting

## 4. Experiment

In order to verify the performance of the algorithm, we develop a surgery navigation system to carry out some experiments. As shown in Fig.5. The system includes optical locator, the skull model and surgery instruments.



(a)



(b)

**Fig. 5.** The hardware equipment of surgery navigation system.  
(a) Optical locator; (b) The skull model and surgery instruments

### 4.1 Instruments Calibration

Firstly, we calibrate binocular camera using Matlab Calib Tool Box [11]. Secondly, we calibrate instruments including probe instrument (Fig.1 (a)) and non-probe instrument (Fig.1(b)). Instruments calibration use 5000 images and the results are used as theoretical true value.

**Table 1.** The calibration result of surgery instruments

	Non-probe instrument	Probe instrument
Distance between marker 1 and 2 (mm)	158.50	106.29
Distance between marker 1 and 3 (mm)	109.35	50.45
Distance between marker 2 and 3 (mm)	114.12	55.85
Distance between marker 1 and pinpoint (mm)		91.20
Distance between marker 2 and pinpoint (mm)		197.48
Distance between marker 3 and pinpoint (mm)		141.64

## 4.2 3-D Reconstruction Accuracy Experiments Of The Surgical Instruments

3-D reconstruction accuracy experiments consist of static accuracy experiments and dynamic accuracy experiments for markers. For simplicity, conventional 3-D reconstruction method is denoted as “C”, conventional 3-D reconstruction method with weighted filter is denoted as “C+W”, 3-D reconstruction of markers based on structure constraints is denoted as “C+S” and 3-D reconstruction of markers based on structure constraints and weighted filter is denoted as “C+S+W”.

### Static accuracy experiments

Surgical instruments static accuracy experiments refer to the differences between reconstruction results and instruments calibration. Surgical instruments are placed statically (Fig. 6). After acquiring over 1000 sets of data and reconstructing the surgical instruments, we calculate the average distances between each marker, the maximum error and mean square error.

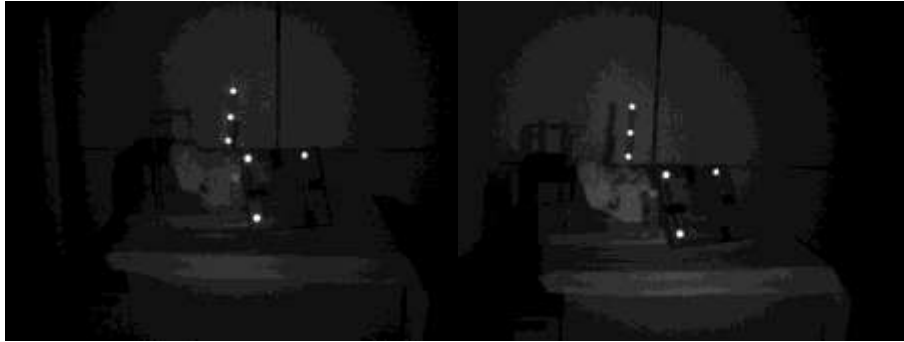


Fig. 6. Put the instruments static

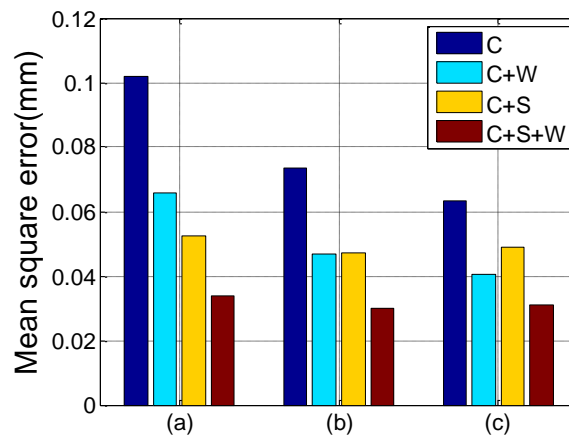
3D reconstruction results of non-probe instrument and the mean square error are shown in Table 2 and Fig. 7 respectively. As shown in Table 2 and Fig. 7, 3-D reconstruction method with weighted filter (“C+W”) can reduce mean square error effectively and 3-D reconstruction of markers based on structure constraints (“C+S”) not only get higher stability, but also makes the reconstruction results closer to theoretical true value. The proposed method (“T+S+W”) reduce the mean square error significantly and get more accurate results.

Table 2. The result of 3-D reconstruction of non-probe instrument

		Mean (mm)	Maximum error (mm)	Mean square error (mm)
C	Distance between marker 1 and 2	159.02	0.34	0.10
	Distance between marker 1 and 3	110.05	0.29	0.07
	Distance between marker 2 and 3	114.16	0.23	0.06
C+ W	Distance between marker 1 and 2	159.02	0.34	0.07
	Distance between marker 1 and 3	110.05	0.19	0.05
	Distance between marker 2 and 3	114.16	0.15	0.04



C+S	Distance between marker 1 and 2	158.73	0.17	0.05
	Distance between marker 1 and 3	109.82	0.18	0.05
	Distance between marker 2 and 3	114.16	0.18	0.05
C+S+W	Distance between marker 1 and 2	158.73	0.17	0.03
	Distance between marker 1 and 3	109.82	0.12	0.03
	Distance between marker 2 and 3	114.16	0.11	0.03



**Fig. 7.** 3D reconstruction of non-probe instrument (a) Distance between mark 1 and 2

(b) Distance between mark 1 and 3 (c) Distance between mark 2 and 3

### Dynamic accuracy experiments

Surgical instruments dynamic accuracy experiments refer to moving the surgical instruments within the scope of SNS and calculating the differences between reconstruction results and instruments calibration. After acquiring over 1000 sets of data and reconstructing the surgical instruments, we calculate the average value of each marker, the maximum error and mean square error.

3D reconstruction results of non-probe instrument and the mean square error are shown in [Table 3](#) and [Fig. 8](#) respectively.

**Table 3.** The result of 3-D reconstruction of the markers on non-probe instrument

		Mean (mm)	Maximum error (mm)	Mean square error (mm)
C	Distance between marker 1 and 2	158.48	2.18	0.26
	Distance between marker 1 and 3	109.33	2.29	0.26
	Distance between marker 2 and 3	114.11	1.38	0.17
C+ W	Distance between marker 1 and 2	158.48	2.14	0.25

	Distance between marker 1 and 3	109.32	2.08	0.26
	Distance between marker 2 and 3	114.11	1.37	0.15
C+S	Distance between marker 1 and 2	158.48	1.16	0.14
	Distance between marker 1 and 3	109.31	1.22	0.19
	Distance between marker 2 and 3	114.11	1.17	0.12
C+S+W	Distance between marker 1 and 2	158.48	1.13	0.13
	Distance between marker 1 and 3	109.31	1.10	0.17
	Distance between marker 2 and 3	114.11	1.11	0.12

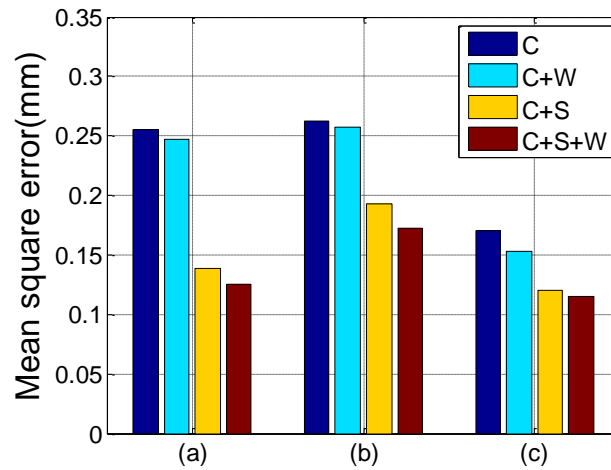


**Fig. 8.** The results of dynamic precision for markers (a) Distance between mark 1 and 2 (b) Distance between mark 1 and 3 (c) Distance between mark 2 and 3

As shown in **Table 3** and **Fig. 8**, 3-D reconstruction method with weighted filter (“C+W”) can reduce mean square error effectively and 3-D reconstruction of markers based on structure constraints (“C+S”) not only get higher stability, but also makes the reconstruction results closer to theoretical true value. The proposed method (“C+S+W”) get the most accurate results.

### 4.3 Probe Reconstruction Accuracy Experiment

Usually, it is hard to get the real coordinates of a point in camera coordinate system and the reconstruction accuracy of it could not be obtained directly. In this experiment, we chose the two ends of a caliper, as shown in **Fig. 9**, and compared the distance of them given by SNS to the real length.

We use the probe type instrument to gain the coordinates of  $P_s$  and  $P_e$  in the camera coordinate system. The real distance between them is 150mm. As shown in **Table 4**, the proposed algorithm whose error is less than 0.5mm outperforms the conventional method.



**Fig. 9.** Probe reconstruction accuracy experiment

**Table 4.** Accuracy experiment of point reconstruction and structure reconstruction

	3-D coord(mm)	C	C+S+W
$P_s$	x	-247.93	-247.61
	y	106.04	106.34
	z	736.30	736.30
$P_e$	x	-97.36	-97.41
	y	106.79	106.62
	z	725.74	727.11
Distance		150.96	150.48

## 5. Conclusion

The accuracy of instrument positioning is very important in SNS. The slightly effects of environment could cause the positioning jitter greatly. This paper presents a method that reconstructing the markers on the surgery instruments as a whole and considers the instruments' structure as a constraint instead of normally reconstructing markers separately. The method calibrates the instruments before navigation to get the structure parameters. Then the information obtained from reconstruction is used in surgery navigation. Furthermore, weighted filter is used to reduce the jitter. In order to verify the performance of the algorithm, we carried out some real data experiments to test the accuracy. The experiment showed that this method improve the accuracy effectively.

## References

- [1] R. Galloway, "The process and development of image-guided procedures", Annual Review of Biomedical Engineering, 2001, 3: 83–108. [Article \(CrossRef Link\)](#)
- [2] R.Taylor, "Summer School Talk - Taylor.pptx - Robotics Summer School", 2012. [Article \(CrossRef Link\)](#)
- [3] Medical Vision Group at the MIT AI Lab, Cambridge, Massachusetts, USA.. [Article \(CrossRef Link\)](#)
- [4] Surgical Planning Laboratory of Bgham and Women's Hospital and Harvard Medical School, Boston, Massachusetts, USA. [Article \(CrossRef Link\)](#)
- [5] D.D. Menthon and L.S. Davis, "New Exact and Approximate Solutions of the

- Three-point Perspective Problem,” Proc. IEEE Int’l Conf. Robotics and Automation, Cincinnati, Ohio, May, 1990, pp.40-45. [Article \(CrossRef Link\)](#)
- [6] J. Yang, and J. Qian, “Research on Computer Aided Surgical Navigation Based on Binocular Stereovision”, Proc. IEEE Int’l Conf. on Mechatronics and Automation, Luoyang, China, June 25-28, 2006, pp.1532-1536. [Article \(CrossRef Link\)](#)
- [7] J. Wang, Digital Infrared Navigator for Surgery, Doctoral Dissertation of Shanghai Jiaotong University, 2007. [Article \(CrossRef Link\)](#)
- [8] Y. Zheng, Y. Liu, “Extent the Projected Sphere Center Deviates from the Perspective Elliptical Contour Center”, IET Electronics Letters, vol.44, no. 11, 673-674, 2008. [Article \(CrossRef Link\)](#)
- [9] R. Hartley and A. Zisserman, “Multiple View Geometry in Computer Vision”, Cambridge, 2004. [Article \(CrossRef Link\)](#)
- [10] Y. Yuan, W. Sun, “Optimization Theory and Methods Science Press”, Beijing ,1997.
- [11] J. Bouguet, Camera Calibration Toolbox for Matlab. [Article \(CrossRef Link\)](#)
- [12] Z. Duan, Z. Yuan, X. Liao, W. Si and J. Zhao. 3D Tracking and Positioning of Surgical Instruments in Virtual Surgery Simulation. Journal of Multimedia, Vol 6, No 6, 502-509, 2011. [Article \(CrossRef Link\)](#)



**Chenhao Wang** received the B.S. degree in Dept. of Automation from Xiangtan University, China, in 2003 and the M.S. degree in Power Electronics & Power Drive from Xiangtan University, China, in 2006. Now he is a Ph.D. student in the Institute of Image Processing and Pattern Recognition, Shanghai Jiao Tong University, China. His current research interests include computer vision and image-guided surgery.



**Yi Shen** received the B.S. degree in Dept. of Automation from Huazhong University of Science and Technology, China, in 2009. Now she is a M.S. student in the Institute of Image Processing and Pattern Recognition, Shanghai Jiao Tong University, China. Her current research interests include image-guided surgery.



**Wenbin zhang** received the Ph.D. degree from the Shanghai Jiao Tong University , in the Department of Oral and maxillo-facial surgery, Shanghai Ninth People’s Hospital, School of Medicine, in 2011, and joined the Oral and Cranio-maxillofacial Science, Shanghai Ninth People’s Hospital, School of Medicine Shanghai Jiao Tong University in 2012 . His research interests are in image-guided surgery and cranio-maxillo-facial surgery.



**Yuncai Liu** received the Ph.D. degree from the University of Illinois at Urbana-Champaign, in the Department of Electrical and Computer Science Engineering, in 1990, and worked as an Associate Researcher at the Beckman Institute of Science and Technology from 1990 to 1991. Since 1991, he had been a System Consultant and then a Chief Consultant of research in Sumitomo Electric Industries, Ltd., Japan. In October 2000, he joined the Shanghai Jiao Tong University as a distinguished Professor. His research interests are in image processing and computer vision, especially in motion estimation, feature detection and matching, and image registration. He also made many progresses in the research of intelligent transportation systems.